DIMENSIONAL EVALUATION OF ADDITIVELY MANUFACTURED PARTS FOR AUTONOMOUS VEHICLES

F. P. Berardi[1,2*], P. H. A. Costa[1], V. B. Mendes[2], M. D. Banea[1,3]

[1]Federal Center of Technological Education in Rio de Janeiro, Brazil
[2] Brazilian Navy Research Institute in Rio de Janeiro, Brazil
[3]CICECO - Aveiro Institute of Materials, Department of Materials and Ceramic Engineering, University of Aveiro, 3810-193, Aveiro, Portugal
*Corresponding author's e-mail address: mdbanea@gmail.com

ABSTRACT

The growing use of drones in civilian and military applications is motivated mainly by reduced costs. Drones, along with autonomous vehicles, require lightweight structures and high dimensional accuracy to improve autonomy and spatial orientation. Additive Manufacturing (AM) enables the production of lightweight parts by controlling internal fill percentages and optimizing the density. However, there is limited research into how the type and percentage of infill affects dimensional tolerance. This study aims to assess the impact of these factors on 3D-printed parts, using low-cost FFF 3D printers with Polylactic Acid (PLA) and Acrylonitrile Butadiene Styrene (ABS) filaments. Overall, the results were satisfactory and met the required tolerances, confirming the feasibility of using parts produced by low-cost 3D printers and commonly available materials in the mass production of drones and autonomous vehicles.

KEYWORDS: drones, autonomous vehicles, additive manufacturing, dimensional tolerance, Fused Filament Fabrication (FFF).

1. INTRODUCTION

With the advance of technology, autonomous vehicles have become capable of carrying out increasingly diverse activities, reducing the exposure of human life to risky situations and allowing us to expand our knowledge of the marine environment [1].

Autonomous vehicles have a wide range of applications in diverse areas such as infrastructure inspection, rescue and emergency operations, logistics and delivery, scientific research, military applications and others. In military applications, the use of Autonomous vehicles is able to contribute as a strong tactical advantage, since they can represent an extension of warships and land vehicles, through the use of Autonomous Underwater Vehicles (AUV) and/or Unmanned Aerial Vehicles (UAV/Drones) [2].

Drones have taken a leading role in counter-terrorism and counter-insurgency and are projected to be of growing importance in future military operations. Their low cost makes them disposable, which is ideal for highly dangerous or politically sensitive missions. However, technical limitations, as well as likely improvements in competing technologies, notably air defence systems, should circumscribe the military role of drones [3].

Based on the study by Ligon et al. [4], it can be seen that 3D printing is widely used in various areas. Among the main applications of 3D printing is the printing of functional parts, which already accounts for around 29% of all use of this technology. In many cases, it is also possible to obtain AM printed products with reliable finishes and structures, so that they can be used as a final product [5]. Thus, 3D printing is demonstrating to be an increasingly relevant technology with the potential to revolutionize the production of end products.

As an example of AM in drone applications, it can be seen in the works presented by Muralidharan et al. [6] and Radharamanan et al., [7] that, in general, the purposes of using AM technology in drone production are weight reduction and topological optimization of the mechanical structure in order to extend the range, reduce the cost of producing prototypes and increase the speed of manufacture. However, some of the difficulties encountered in designing, building, testing and flying a drone using 3D printers include assembly errors, sizing problems and software incompatibility [7]. The initial estimate of the route deviation of autonomous vehicles must include error contributions from both the Inertial Measurement Units (IMU) and the mechanical system that maintains it in the required position during operation. Understanding the impact that these errors have on the main functions of a

http://doi.org/10.35219/awet.2024.03
Date of submission/acceptance: 31.05.2024/15.12.2024

navigation system helps to set relevant performance targets that avoid overloading the problem while managing the risk of losing key performance and cost trade-offs [8].

Recent studies have investigated the dimensional accuracy of 3D printed parts using FFF technology. Grgić et al. [9], developed a novel method based on ISO 286 to achieve dimensional accuracy for assembly-fit parts, finding optimal parameters for horizontal expansion and linear advance. Zemicik and Sedlak [10] highlights the complexity of the printing process, emphasizing the wide range of parameters and limits. Drozda et al. [11], for example, state that for FFF technology, a complete and systematic analysis of precision, tolerance and repeatability is essential. Schaechtl et al. [12] highlighted imperfections such as joint gaps and geometric deviations that depend on machine-specific process parameters. However, it was shown that a relatively simple reference part can be a good option for effectively assessing the accuracy of various geometric features and revealing differences between two desktop 3D printers in terms of accuracy [13].

An investigation into the influence of layer thickness and filler density on the geometric tolerance of parts produced by FFF is presented in [14]. However, this study was carried out only for the Nylon material and used a machine that is more expensive than the one used in this work. Therefore, this article aims to evaluate the consistency of dimensional accuracy in parts produced by a 3D printer for use as final components in mechanical structure assemblies. The study seeks to confirm the feasibility of employing low-cost 3D printers and commonly available materials in the mass production of autonomous vehicles.

2. MATERIALS AND METHODS

The 3D printing process flows from the creation of a three-dimensional model using CAD (Computer-Aided-Design) software [16]. This model is converted into a file in stereolithography (STL) format, which simplifies the original model into a set of triangular elements.

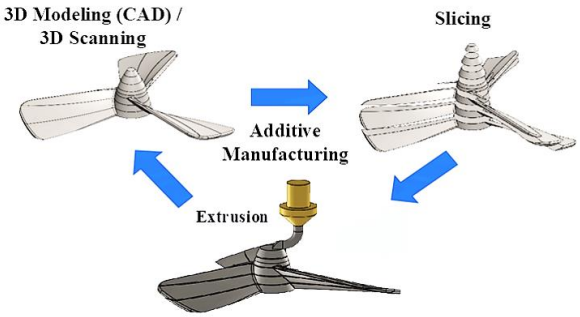

Fig. 1. Basic concept of the AM process

This file is then divided horizontally (or sliced) using slicing software into several layers (Fig. 1), representing the two-dimensional contours, which when deposited on top of each other using a process called FFF form the original three-dimensional model [17].

Before presenting the methodology used for this study, it is important to provide information on the instrumentation used, some definitions regarding the parameters for generating specimens and the dimensional inspection procedure adopted.

2.1. Instrumentation

The same instrumentation used by Grgić et al. [9] was taken as the basis for this article. That is, the CREALITY ENDER-3 PRO 3D printer with an accuracy of ±0.1 mm, the CURA slicing software, version 5.7.1 and the PLA filament (grade A - 100% original, and innocuous material, white, 1, 75mm). In this work, an investigation for ABS filament (grade A - 100% original, and harmless material, white, 1.75 mm) was also added. It is important to highlight that both materials are in accordance with the specifications of the manufacturer 3D LAB. Research based on these materials is interesting because they are easily available on the market, affordable and can be used in a variety of applications. In addition, these materials were characterized in tensile and flexural tests, in accordance to ASTM standards, to investigate and compare the mechanical properties of the AM parts as a function of material used [18].

Other important observations have been reported about these materials, PLA has excellent mechanical properties, thermal stability, good processing capability, and low environmental impact. However, one disadvantage is that PLA is relatively expensive compared to other petroleum-based polymers [19]. ABS thermoplastic material has good mechanical properties, but it emits an unpleasant odour during processing [20]. However, novel materials for 3D printing are continuously being developed. Thus, in order to further understand the mechanical properties of these AM materials and stimulate their use in new applications in the industry, more research work is needed [18].

The specimens were designed and manufactured at the Prototyping Laboratory (LabProM) of the Brazilian Navy Research Institute. The dimensional inspection was carried out at the Metrology Laboratory of the Brazilian Navy Research Institute. All measurements were obtained using a Mitutoyo B-251 three-dimensional machine, last calibrated on 22/09/2022, containing the MCOSMOS-Manual v3.0 R3 Edition 17 software.

2.2. Designation of the specimen

This section presents the details and considerations taken as decision criteria to determine the parameters

considered in the definition of the specimen model.

2.2.1. Printing improvements

As guided by Grgić et al. [9], the extruder's material flow was calibrated by adjusting the step/mm ratio and levelling the table.

2.2.2. CAD model and STL file conversion

Based on the specimen model used by Grgić et al. [9], a torus with an internal diameter of 35 mm, an external diameter of 50 mm and a height of 10 mm was adopted for the three-dimensional implementation of the specimen in the Solidworks 2022 program, as shown in figure 2.

According to reference Grgić et al. [9], it can be seen that the refinement of the triangular mesh in the STL file influences the dimensions of circular objects. Therefore, to convert the CAD file to STL, the Solidworks program settings were customized for maximum resolution, with tolerance values of 0.0035mm for the "Deviation" parameter and 0.5º for the angle (Fig. 3).

2.2.3. Slicing process

Based on the standard parameters of the CURA program, a preliminary analysis of the slicing parameters to be adopted in the manufacture of the specimen was carried out, implementing the changes proposed by Ref [9]. The parameters for specimen 01 are shown in table 1.

Specimens 02 was then produced, changing the Linear Advance parameter to 25 and specimens 03, with Linear Advance of 25, Initial Horizontal Expansion of -0.2mm and Hole Size of 0.13mm, which were the resources used by [9]. By comparing the dimensions of these specimens at two different heights, it was possible to conclude that the parameters used by [9] were indeed the ones that produced specimens with dimensions closest to those of the CAD model. With this, the parameters for the production of the subsequent specimens were determined (Table 2).

Regarding the percentage of internal filling, this study evaluated two extreme cases: 100%, representing the maximum setting, and 20%, the default value in the CURA program. This approach allowed for a comparative analysis of these contrasting scenarios. For the fill pattern, the line, grid, and gyroid types were selected arbitrarily for evaluation.

2.2.4. 3D printing

The specimens were manufactured on the Ender 3 Pro 3D printer, using 3D Lab PLA and ABS filaments, in a room with a monitored environment, with a temperature between 23 and 28ºC and humidity between 44 and 64%.

In addition, to make it easier for the specimen to adhere to the table during extrusion, Scotch brand glue sticks made of polyvinyl were used.

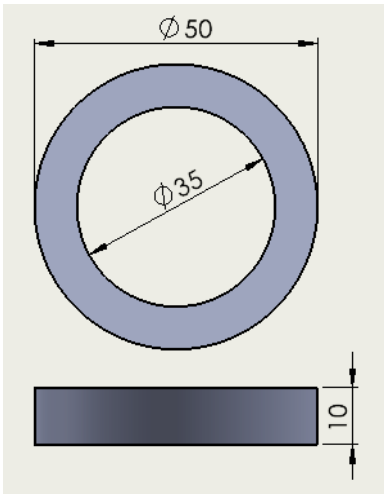

Fig. 2. Three-dimensional model of the specimen

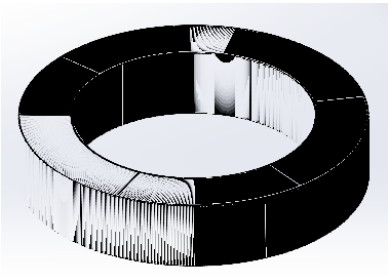

Fig. 3. High resolution STL model of the specimen

Table 1. Specimens 01 printing parameters

Printing Parameters	**PLA**
Extrusion temperature [°C]	200
Table temperature [°C]	60
Internal Filling [%]	100
Type of Filling	Line
Filling orientation	45°
Linear Advance	0
Initial Horizontal Expansion [mm]	0
Hole size [mm]	0
Ambient temperature [°C]	27
Humidity [%]	44
Start of Layer	Posterior

.

Table 2. Specimen printing parameters

Printing Parameters	**PLA**	**ABS**
Extrusion temperature [°C]	200	230
Table temperature [°C]	60	100
Height between nozzle and table [mm]	0.2	0.2
Filament diameter [mm]	1.75	1.75
Internal Filling [%]	20 and 100	20 and 100
Type of Filling	Line, Grid and Gyroid	Gyroid
Filling orientation	45°	45°
Print speed [mm/s]	50	50
Extrusion nozzle diameter [mm]	0.4	0.4
Linear Advance	25	25
Initial Horizontal Expansion [mm]	-0.2	-0.2
Hole size [mm]	13	13
Ambient temperature [°C] and Humidity [%]	23 to 28/ 44 to 65	23 to 28/50 to 65
Start of Layer	Posterior	Posterior

2.3. Dimensional inspection

The dimensional survey of the parts took place in the Metrology Laboratory of the Brazilian Navy Research Institute, in a monitored environment with a temperature of 22°C and humidity between 45 and 60%. The measurement procedure for each dimension, internal and external diameter, was carried out by contacting the tool at four equidistant points at two different heights on the specimens, as shown in Fig. 4.

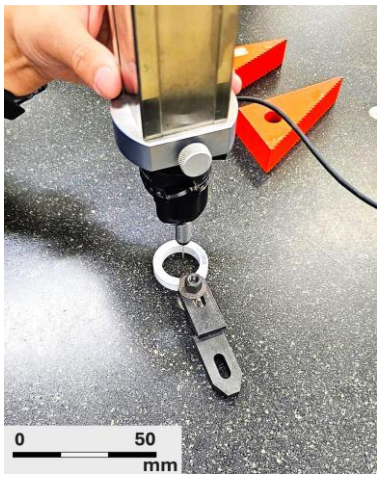

Fig. 4. Three-dimensional-machine contact point

Measuring each dimension at two different heights is necessary due to the possible presence of the "elephant's foot" printing error, which corresponds to a dimensional variation that can occur at the base of the parts, resulting in an increase in dimension for external shaft measurements and a decrease for internal hole measurements. This discrepancy can occur due to the adjusted distance between the extruder nozzle and the printing table, which leads to compression of the material deposited in the first layers, causing the material to spill out laterally [9], as can be seen in figure 5.

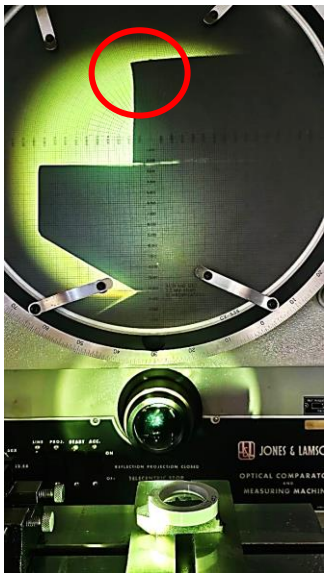

Fig. 5. Model printed on a profile projector showing the "Elephant's Foot" anomaly

In this way, two heights were defined to be evaluated on the specimens (Fig. 6), the first with a height H1 = 1 mm, close to the first layers to evaluate the effect of the "elephant's foot", and the second H2 = 8 mm, far enough from the base to ensure that the "elephant's foot" does not significantly affect the nominal dimension of the specimens. Both measurements are referenced to the base of the printing table.

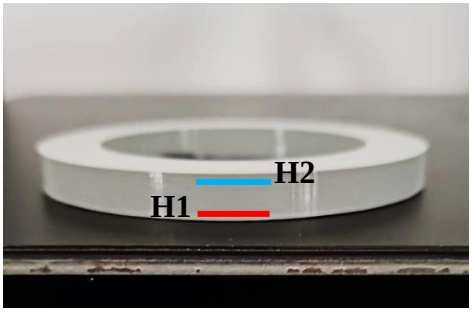

Fig. 6. H1 (red line) and H2 (blue line): Heights with and without of the "elephant's foot" effect, respectively

2.4. Research methodology

For this study, the investigation procedure was to measure the dimensions of three standard specimens for each type (Line, Grid and Gyroid) and percentage (20 and 100%) of filling, as shown in figure 2. The average and standard deviation of the dimensions of the inner and outer diameters at heights H1 and H2 were checked for each specimen and then compared to see if they fell within the Dimensional Tolerance range of the DIN 7168 Standard, which is above 30 mm up to 120 mm with permissible deviations of 0.3 mm. The layout of the specimens produced can be seen in the flowchart shown in figure 7.

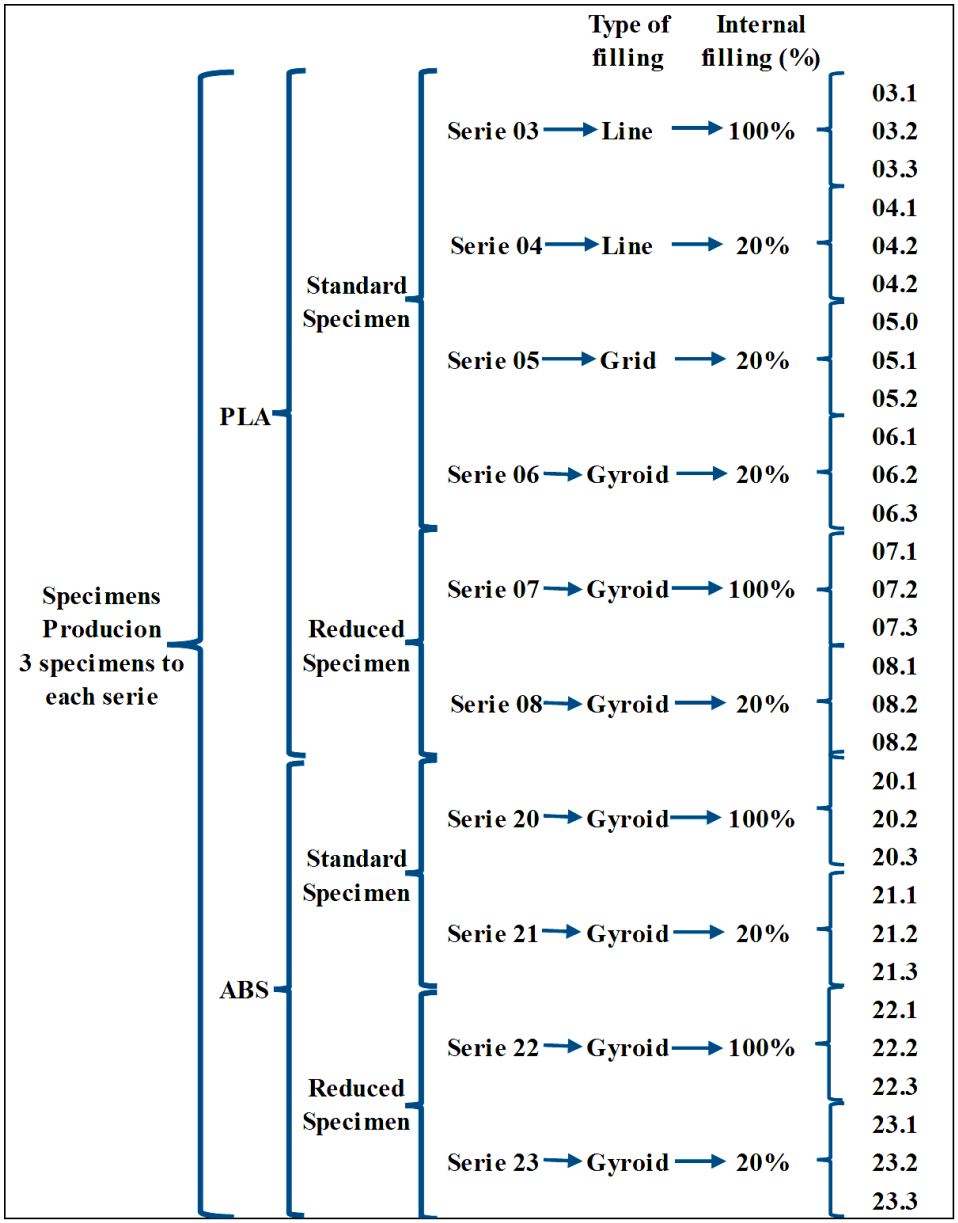

Fig. 7. Flowchart of the specimens

In addition, a new evaluation was carried out by changing the external and internal diameters, reducing the values to half the initial value of specimen 03, as presented in figure 8.

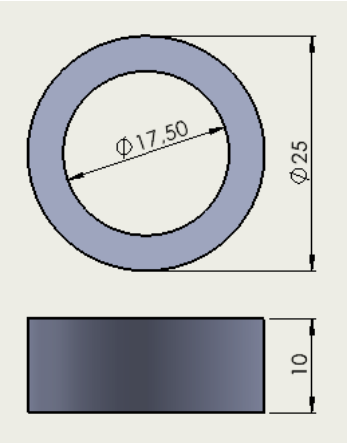

Fig. 8. Reduced specimen model

Thus, with the specimens reduced, the dimensions of the outer and inner diameters fall within another range of Dimensional Tolerance of the DIN7168 Standard - Medium Grade, over 6 mm up to 30 mm with permissible deviations of 0.2 mm, which makes it possible to check whether the tolerances behave in relation to the order of magnitude of the dimensions.

For the specimens with smaller diameters, it was decided to evaluate only those produced in the percentage of 20% in the Gyroid pattern, as this was the pattern that showed the greatest discrepancy in relation to the nominal dimension of the CAD model in the initial investigation, and also with a percentage of 100% filling.

3. RESULTS

All the specimens had their internal and external diameters measured at the defined heights (H1 and H2), and then the average and standard deviation of each series was calculated. To illustrate the procedure for investigating the data collected, the values obtained for the H2 measurements of the specimens 03 series are shown in table 3.

From table 3 it can be seen that the average of the specimen 06 series, with a gyroid filling type, is furthest away from the average of the specimen 03 series for internal diameter, with a difference of 0.07 mm and 0.155 for the nominal value of 35 mm, but both also fall within the DIN 7168 - Medium Grade tolerance. It is also interesting to note that the difference is even smaller in the case of the outer diameter. It is also worth noting that the biggest difference between the specimen series measurements is 0.035 mm and the difference to the nominal value of 50 mm is 0.139 mm. Another important piece of information to note is that the specimen series with total filling has a larger outer diameter and a smaller inner diameter than the other series, probably due to the excess material deposited.

Table 4 shows the average values of the series of solid specimens (100% fill) and the series of specimens with 20% fill and with the patterns: Line, Grid and Gyroid.

Table 3. Results of the specimens 03 series

Coding	H2		Internal Filling (%)	Type of Filling
	Int. D. (mm)	Ext. D. (mm)		
Specimen 03.1	35.079	49.785	100	Line
Specimen 03.2	35.031	49.878	100	Line
Specimen 03.3	35.014	49.839	100	Line
Average Specimen 03.1, 03.2, 03.3	35.041	49.834	100	Line
Standard Deviation	0.040	0.039		

Table 4. Averages and standard deviation - averages 03, 04, 05 and 06

Coding	H2		Internal Filling (%)	Type of Filling
	Int. D. (mm)	Ext. D. (mm)		
Average Specimen 03.1, 03.2, 03.3	35.085	49.896	100	Line
Standard Deviation	0.040	0.039		
Average Specimen 04.1, 04.2, 04.3	35.107	49.861	20	Line
Standard Deviation	0.023	0.007		
Average Specimen 05.1, 05.2, 05.3	35.124	49.871	20	Grid
Standard Deviation	0.031	0.020		
Average Specimen 06.1, 06.2, 06.3	35.155	49.884	20	Gyroid
Standard Deviation	0.041	0.013		

Figures 9a, 9b, 10a and 10b show the average values for the diameters of the specimens from the initial investigation, with a standard size, and the smaller specimens with a 50% reduction in diameter. In this way, it is possible to assess the tolerance relationship in another order of magnitude range.

Figures 9a and 10a show that the standard size series (specimens 03 and specimens 06) vary by 0.07 mm and 0.012 mm for the internal and external diameters, respectively, while the reduced specimens series do not. Figures 9b and 10b, on the other hand, show a variation of 0.043 mm and 0.058 mm. As a result, it is not possible to observe a direct relationship between the tolerance and the order of magnitude of the measurements, but rather the same behaviour in the variation of the larger outer diameter and smaller inner diameter in the case of the solid specimens compared to the other specimens.

The same study was carried out for the ABS material and is shown in figures 11a, 11b, 12a and 12 b, where it is possible to observe a similar behaviour to PLA. However, it should be noted that all the averages of the ABS material series are lower than the averages of their respective PLA material series.

In general, although all the results are within the tolerance recommended by DIN7168 Medium Grade standards, the standard deviation of the specimens is a maximum of 0.075mm.

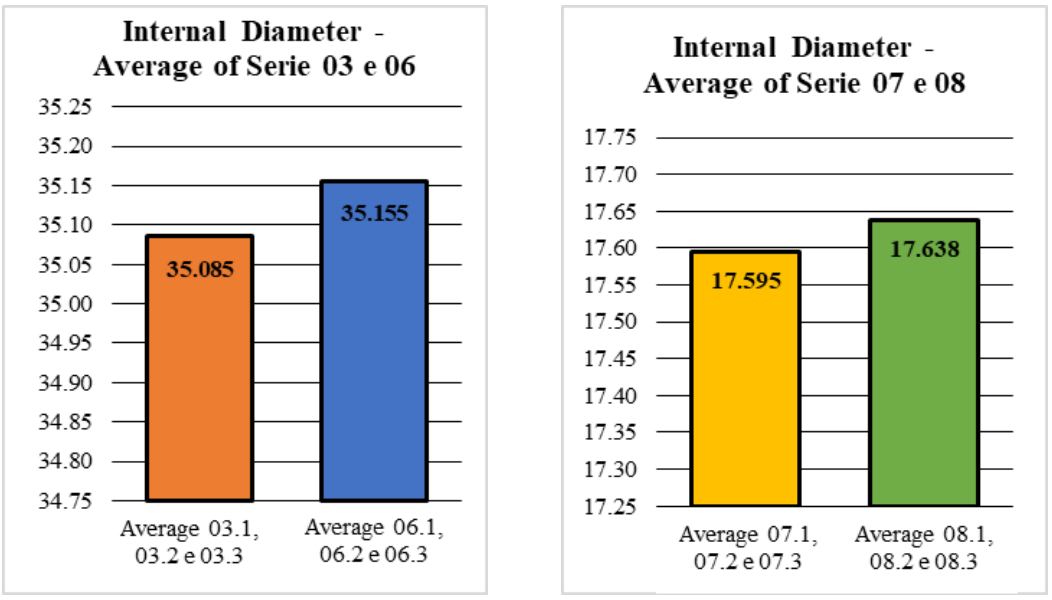

a) b)

Fig. 9. Internal diameter data PLA: a) standard specimen PLA and b) reduce specimen PLA

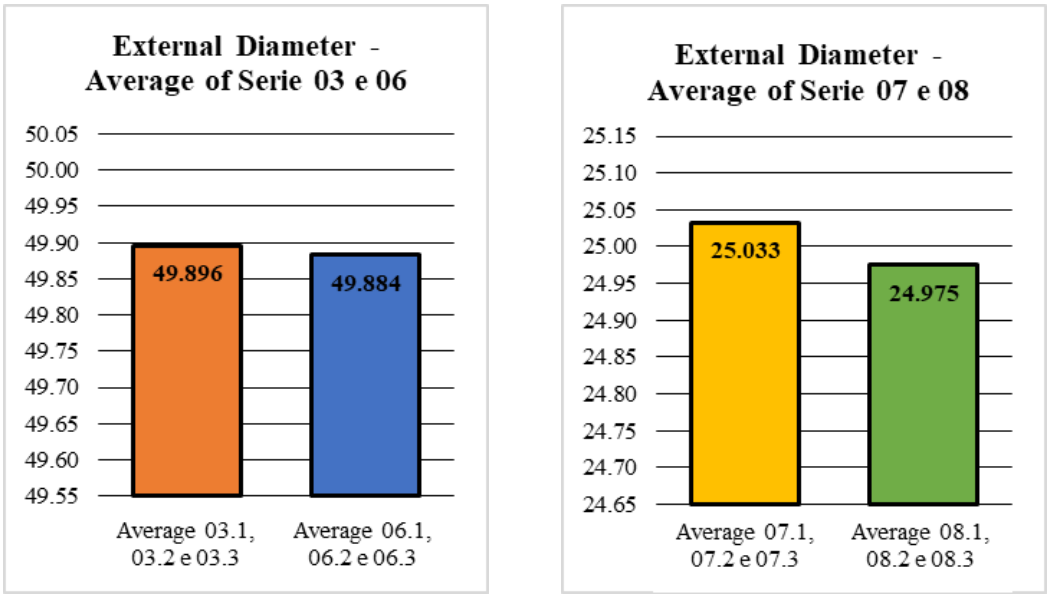

a) b)

Fig. 10. External diameter data PLA: a) standard specimen PLA and b) reduce specimen PLA

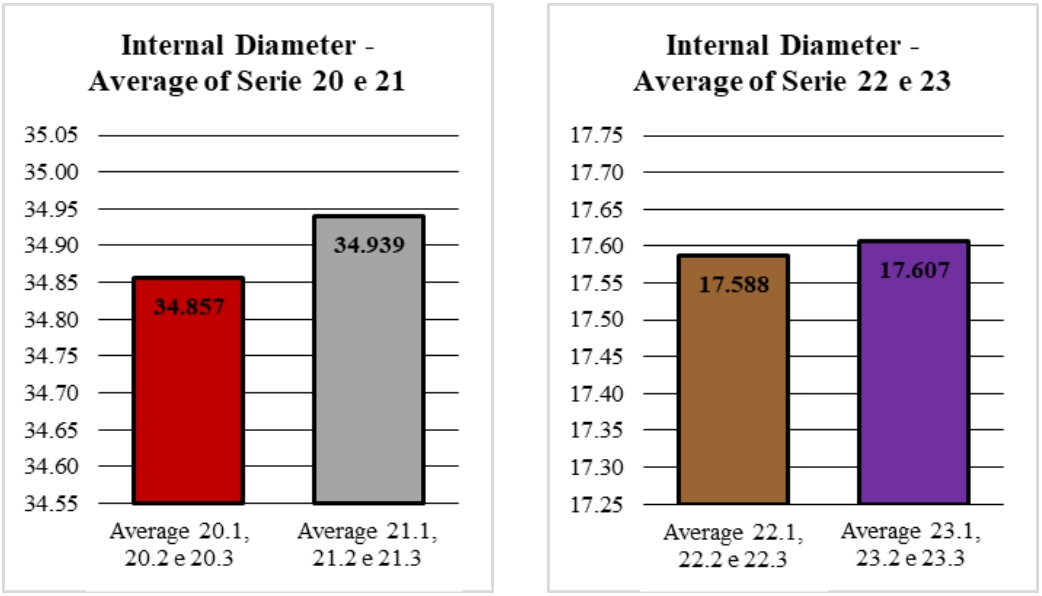

a) b)

Fig.11. Internal diameter data ABS: a) standard specimen ABS and b) reduce specimen ABS

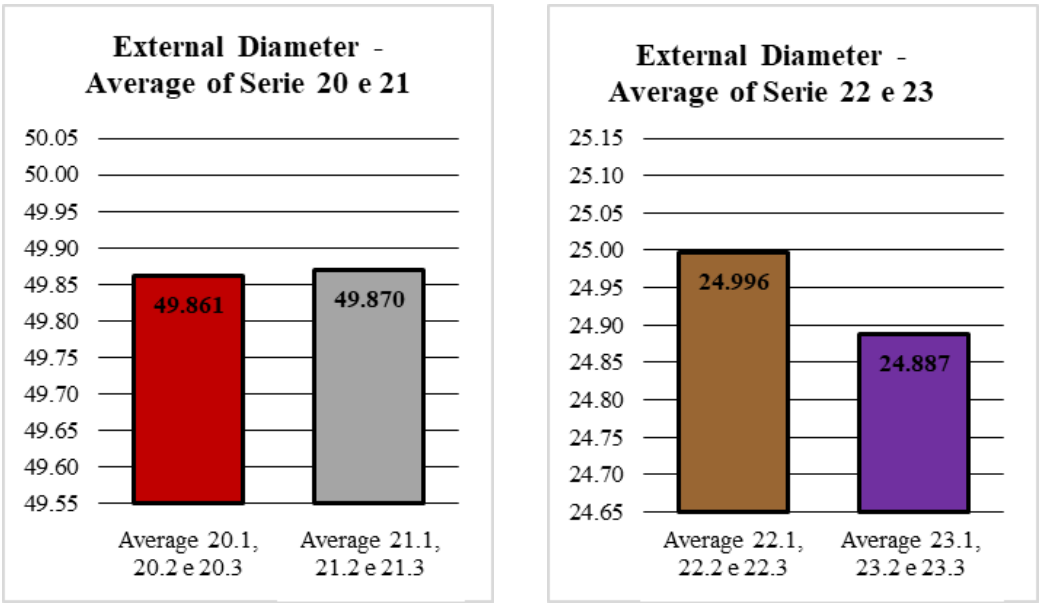

a) b)

Fig. 12. External diameter data ABS: a) standard specimen ABS and b) reduce specimen ABS

4. CONCLUSIONS

Based on the findings presented in this article, it can be concluded that it is feasible to produce series-manufactured components for final products using low-cost 3D printing machines and readily available materials. These components meet the dimensional requirements outlined in the DIN 7168 Medium Grade tolerance table. Consequently, their application in the mechanical structures of autonomous vehicles could offer significant value, particularly in politically sensitive scenarios.

In addition, the results presented confirm what was reported in the literature, i.e., that ABS material has a higher compression rate than PLA, and that solid printed parts tend to expand by increasing the external diameter and decreasing the internal diameter. Although the measurements obtained comply with the DIN 7168 Medium Grade standards, it is possible to achieve dimensions closer to nominal values by addressing systematic errors, such as those introduced during the three-dimensional modelling of the specimens. To meet the stricter requirements of DIN 7168 Fine Grade, further research should explore alternative materials and printing parameters. Future studies will also focus on the dimensional evaluation of additional geometric shapes.

Environmental factors, such as temperature and humidity during the additive manufacturing (AM) process, can significantly impact dimensional stability. Variations in ambient temperature may lead to uneven cooling and thermal stresses, while fluctuations in

humidity can affect the material properties of hygroscopic polymers like PLA investigated here. A study of these variables would provide a deeper understanding of their influence on dimensional accuracy and part quality and will be considered in the future.

ACKNOWLEDGEMENTS

Authors would like to acknowledge the support of the Mechanics Prototyping Laboratory, the Metrology Laboratory, both of the Brazilian Navy Research Institute, and the Federal Center of Technological Education (CEFET/RJ).

REFERENCES

[1] **Dunbabin M., Marque L.,** *Robotics for Environmental Monitoring,* [From the Guest Editors], IEEE Robotics & Automation Magazine, IEEE, v. 19, n. 1, 2012, pp. 20–23.
[2] **W. H. Adnan, et al.,** *Drone Use in Military and Civilian Application: Risk to National Security*, Journal of Media and Information Warfare, v. 15(1), pp. 60-70, 2022.
[3] **P. Mahadevan,** *The Military Utility of Drones*, CSS Analyses in Security Policy V.78, Center for Security Studies (CSS), ETH Zurich, 2010.
[4] **S. C. Ligon, et al.,** *Polymers for 3D printing and customized additive manufacturing*, Chemical Reviews, n. 117, pp. 10212–10290, 2017.
[5] **E. C. Mendonça, et al.,** *Desenvolvimento de um veículo submarino autônomo de baixo custo utilizando manufatura aditiva*, Revista Pesquisa Naval, n. 32, pp. 10-16, 2020.
[6] **N. Muralidharan, et al.,** *Structural analysis of mini drone developed using 3D printing technique*, Materials Today: Proceedings, n. 46, pp. 8748–8752, 2021.
[7] **R. Radharamanan, et al.,** *Use of 3D Printers to Design, Build, Test and Fly a Quadcopter Drone*, The Journal of Management and Engineering Integration Vol. 9, No. 1, 2016.
[8] **M. Looney,** *The Basics of MEMS IMU/Gyroscope Alignment*, Analog Dialogue p. 49-06, June 2015.
[9] **I. Grgić, et al.,** *Accuracy of FDM PLA Polymer 3D Printing Technology Based on Tolerance Fields*, Processes 2023, 11, 2810, 2023.
[10] **O. Zemicik, J. Sedlak,** *Application of Linear Optimization on Parameters of 3D FDM Print*, Tehnicki vjesnik - Technical Gazette, v. 26, n. 4, jul. 2019.
[11] **F. O. Drozda, T.R. Pereira, A. E. Patterson,** *End-User Manufacturing with FDM/FFF: Interfaces, Tolerances, Repeatability, and Dimensional Accuracy*, 2020 IISE Annual Conference and Exhibition, New Orleans, LA, USA, 2020.
[12] **P. Schaechtl, B. Schleich, and S. Wartzack,** *Statistical Tolerance Analysis of 3D-Printed Non-Assembly Mechanisms in Motion Using Empirical Predictive Models*, Applied Sciences, v. 11, n. 4, p. 1860, 20 fev. 2021.
[13] **J. Kacmarcik, et al.,** *An investigation of geometrical accuracy of desktop 3D printers using CMM*. IOP Conference Series: Materials Science and Engineering, v. 393, p. 012085, 10 ago. 2018.
[14] **P. Pombinha, et al.,** *A Study on the Effect of Layer Thickness and Infill Density on Geometric Tolerance in Fdm*, 3rd International Conference on Progress in Additive Manufacturing (Pro-AM 2018), Singapore, p. 14–17, May 2018.
[15] **DIN 7168,** *General tolerances for linear and angular dimensions and geometrical tolerances*, DIN Deutsches Institut für Normung e. V., Berlin, 1991.
[16] **A. A. Gorni,** *Introdução a prototipagem rápida e seus processos*, Revista Plástico Industrial, p. 230–239, 2001.
[17] **S. Ahn, et al,** *Anisotropic material properties of fused deposition modelling ABS*. Rapid prototyping journal, 2002.
[18] **Cavalcanti D. K. K., Banea M. D., de Queiroz H. F. M.,** *Effect of material on the mechanical properties of additive manufactured thermoplastic part*. Annals of Dunarea de Jos University of Galati Fascicle XII, Welding Equipment and Technology, vol. 31, 2020, pp. 5-12.
[19] **Carrasco F., Pagès P., Gámez-Pérez J., Santana O. O., Maspoch M. L.,** *Processing of poly(lactic acid): characterization of chemical structure, thermal stability and mechanical properties*, Polymer Degradation and Stability, vol. 95, 2010, pp. 116-125.
[20] **Ngo T. D., Kashani A., Imbalzano G., Nguyen K. T. Q., Hui D.,** *Additive manufacturing (3D printing): A review of materials, methods, applications and challenges*, Composites Part B: Engineering. vol. 143, 2018, pp. 172-196.